Photolysis of pyruvic acid in ice: Possible relevance to CO and CO_2 ice core record anomalies

M. I. Guzmán,[1] M. R. Hoffmann,[1] and A. J. Colussi[1]

Received 4 August 2006; revised 19 January 2007; accepted 28 January 2007; published 26 May 2007.

[1] The abnormal spikes detected in some CO and CO_2 polar ice core records indicate persistent chemical activity in glacial ice. Since CO and CO_2 spikes are correlated, and their amplitudes scale with reported CO/CO_2 yields for the photolysis of dissolved natural organic matter, a common photochemical source is implicated. Given that sufficient actinic radiation is constantly generated throughout ice by cosmic muons (Colussi and Hoffmann, 2003), it remains to be shown that the photolyses of typical organic contaminants proceed by similar mechanisms in water and ice. Here we report that the photodecarboxylation of pyruvic acid (PA, an ubiquitous ice contaminant) indeed leads to the same products nearly as efficiently in both media. CO_2 is promptly released from frozen PA/H_2O films upon illumination and continues to evolve after photolysis. By analogy with our studies in water (Guzmán et al., 2006b), we infer that ^{3}PA* reacts with PA in ice producing $CH_3C(O)C(O)O\cdot$ and ($CH_3\dot{C}$ (OH)C(O)OH) radicals. The barrierless decarboxylation, $CH_3C(O)C(O)O\cdot \rightarrow CH_3C(O)\cdot + CO_2$, accounts for prompt CO_2 emissions down to ~140 K. Bimolecular radical reactions subsequently ensue in fluid molecular environments, both in water and ice, leading to metastable intermediates that decarboxylate immediately in water, but protractedly in ice. The overall quantum yield of CO_2 production in the λ ~313 nm photolysis of PA in ice at 250 K is ~60% of that in water at 293 K. The in situ photolysis of natural organic matter is, therefore, a plausible explanation of CO and CO_2 ice core record anomalies.

Citation: Guzmán, M. I., M. R. Hoffmann, and A. J. Colussi (2007), Photolysis of pyruvic acid in ice: Possible relevance to CO and CO_2 ice core record anomalies, *J. Geophys. Res.*, *112*, D10123, doi:10.1029/2006JD007886.

1. Introduction

[2] Gas bubbles trapped in deep ice could be intact remnants of Earth's paleoatmospheres [*Brook*, 2005; *EPICA*, 2004; *Fischer et al.*, 1999; *North Greenland Ice Core Project Members*, 2004; *Stauffer*, 2000; *Wolff*, 2005]. If so, the correlation of CO_2 concentrations in ancient ice bubbles with the coeval ambient temperatures reported by ^{18}O or ^2H abundance in the enclosing ice [*Brook*, 2005; *Landais et al.*, 2006] would be a significant (although perhaps not definitive) [*Boucot and Gray*, 2001; *Mudelsee*, 2001; *Pearson and Palmer*, 2000] precedent to the potential climatic effects of contemporary anthropogenic CO_2 emissions.

[3] Air extracted from polar ice registers atmospheric CO_2 concentrations that have risen exponentially (from preindustrial ~280 ppmv levels) during the last two centuries. Notice that even higher CO_2 concentrations attended the transition from the last glaciation period to the Holocene [*Tschumi and Stauffer*, 2000]. Ominously, however, some records appear to be tainted by uncharacterized in situ processes. For example, Siple Dome CO_2 ice core records contain anomalous sections that are not replicated in other Antarctic sites [*Ahn et al.*, 2004]. Furthermore, Greenland records dating from the last two millenia display CO_2 concentrations that exceed (by up to ~20 ppmv) those in coeval Antarctic sites [*Anklin et al.*, 1995; *Haan and Raynaud*, 1998]. These discrepancies (1) are localized in thin sections representing less than two annual periods, i.e., much shorter than the decadal intervals elapsing between snow deposition and gas encapsulation, (2) are larger than the precision of measurements (±3 ppmv), and (3) cannot be ascribed to interhemispheric gradients [*Stauffer et al.*, 2002]. The international scientific community justifiably awaits a plausible explanation of this outstanding paleoclimatic issue.

[4] The irregular records reflect chemical activity under conditions that apparently exclude such possibility, because the production of carbon oxides requires their precursors to react while frozen at approximately −35°C, at hundreds of meters below the surface, in the complete absence of sunlight. Several mechanisms have been proposed to account for this phenomenon. It has been speculated that CO_2 could originate from the acidification of carbonate [*Delmas*, 1993; *Stauffer et al.*, 1998] or the oxidation of organic matter by coextensive oxidizers, such as H_2O_2 [*Tschumi and Stauffer*, 2000].

[5] The likelihood that CO_2 spikes originate from the acidification of carbonates can be tested by comparing CO_2 versus carbonate profiles in ice cores, as proposed by *Anklin*

[1]Environmental Science & Engineering, California Institute of Technology, Pasadena, California, USA.

0148-0227/07/2006JD007886

et al. [1995] Such test has now been performed at Dome Fuji, East Antarctica, where CO_2 was found to be uncorrelated with either Ca^{2+}, a proxy for carbonate, or acidity [*Kawamura et al.*, 2003]. Kawamura et al. estimate, from their measurements, that only 2–4% of the 10–20 ppmv excess CO_2 detected in 17–22 kyr old sections could have originated from the in situ acidification of carbonate [*Kawamura et al.*, 2003].

[6] The putative thermal oxidation of easily oxidizable aldehydes by H_2O_2 [*Haan and Raynaud*, 1998; *Tschumi and Stauffer*, 2000] is chemically unlikely for kinetic and mechanistic reasons. The uncatalyzed oxidation of formaldehyde by H_2O_2 (1) with an activation energy E_a = 36 kJ mol^1 is a slow reaction [$\exp(E_a / RT) = 1.4 \times 10^8$ at 240 K] [*Do and Chen*, 1994] and (2) in aqueous solution yields carboxylic acids (e.g., formic acid from formaldehyde) that are quite resilient to further oxidation, instead of carbon oxides [*McElroy and Waygood*, 1991; *Satterfiled and Case*, 1954]. The detection of unreacted H_2O_2 [*Hutterli et al.*, 2003; *Sigg and Neftel*, 1991] and organic matter in close proximity within ice cores after thousands of years further undermines this proposal [*Tschumi and Stauffer*, 2000]. Finally, the large activation energy ($E_a \sim 110$ kJ mol^1) [*Price and Sowers*, 2004] associated with the metabolic activity of psycrophilic microbes drastically caps production rates of catabolic gases (such as CO_2 and CH_4) in anomalous ice core sections, which are much shallower and colder ($T < -35$°C down to ~1000 m depths) than Lake Vostok dome (nearly 4000 m deep) [*Price et al.*, 2002].

[7] Since CO cannot be produced by acidifying carbonate, the fact that some CO records are also exceedingly irregular [*Haan and Raynaud*, 1998] is a significant clue. The nearly constant ~50 ppbv CO levels detected in the Vostok (Antarctica) ice core are not replicated by Eurocore (Greenland) readings, which display greater variability and reach up to 180 ppbv in layers antedating ~1500 AD [*Haan et al.*, 1996; *Haan and Raynaud*, 1998; *Tschumi and Stauffer*, 2000]. Even more revealingly, Eurocore ice core CO and CO_2 profiles exhibit similar trends [*Haan and Raynaud*, 1998]. The latter observation strongly suggests a common source of contamination that, as a further constraint, should generate CO and CO_2 in ~1:100 ratios.

[8] At variance with thermal bimolecular thermal reactions, photochemical transformations are temperature-independent unimolecular events. The possibility of photochemistry in deep ice has been unwittingly disregarded in the past, however, due to the lack of conceivable sources of in situ actinic radiation. The detection of ultraviolet radiation generated by penetrating muons of cosmic origin in deep Antarctic ice [*Andres et al.*, 2001; *Burden and Hieftje*, 1998; *Cowen et al.*, 2001] and the finding that Greenland ice cores are significantly contaminated with organic matter from medieval boreal forest fires [*Kawamura et al.*, 2001; *Savarino and Legrand*, 1998] lend verisimilitude to a photochemical mechanism [*Colussi and Hoffmann*, 2003].

[9] Humic and humic-like substances [*Gao and Zepp*, 1998; *Johannessen and Miller*, 2001; *Kieber et al.*, 1989; *Mopper et al.*, 1991; *Moran and Zepp*, 1997; *Opsahl and Zepp*, 2001; *Valentine and Zepp*, 1993; *Zuo and Jones*, 1996], widespread in natural waters, atmospheric aerosol, and polar ice [*Calace et al.*, 2001; *Grannas et al.*, 2006; *Grannas et al.*, 2004; *Grannas et al.*, 2002; *Kawamura et al.*, 2005; *Kawamura et al.*, 2003; *Kawamura et al.*, 2001] are known to be photodegraded by sunlight into CO and CO_2 in ~1:50 ratios, which are tantalizingly commensurate with their relative excesses in anomalous ice core records (vide supra). The preceding analysis suggests that the photodecomposition of humic-like chromophores sporadically injected as contaminants into glacial ice is potentially able to simultaneously explain CO and CO_2 anomalous spikes.

[10] Organic photochemistry in ice is, however, a largely unexplored subject. More specifically, information is lacking about whether a typical photodecarboxylation reaction would proceed by the same mechanism and produce CO_2 in similar quantum yields in ice and water. Here we report a comparative study of the photodecarboxylation of the environmentally ubiquitous pyruvic acid (2-oxopropanoic, PA) [*Kawamura et al.*, 2001] in fluid and frozen aqueous solutions, reaction (1) [*Budac and Wan*, 1992; *Guzmán et al.*, 2006a; *Guzmán et al.*, 2006b; *Wan and Budac*, 1995]:

$$CH_3C(O)C(O)COH + h\nu \rightarrow\rightarrow CO_2 + \text{other products} \quad (1)$$

which provides factual support to our hypothesis.

2. Experimental Section

[11] One hundred millimolar PA (Aldrich 98.0%, bidistilled at reduced pressure) solutions in Milli-Q water were acidified to pH 1.0 with perchloric acid (Mallinckrodt, 70% analytical reagent) prior to photolysis to ensure that all (>98%) of the photogenerated CO_2 would be released into the gas-phase after thawing the photolyzed samples. It should be emphasized that the photolysis of PA (pK_a = 2.39) actually involves the undissociated acid rather than its anion [*Leermakers and Vesley*, 1963]. We confirmed that quantum yields of PA [*Closs and Miller*, 1978] and benzoylformic acid (BF) [*Gorner and Khun*, 1999] photodecarboxylations are independent of photolyte concentration. Fluid or frozen solution samples (4 mL) were photolyzed in a reactor consisting of a cylindrical chamber fitted with an axial silica finger housing a UV pencil lamp (Hg Pen-Ray model CPQ 8064, emitting at 313 ± 20 nm) and connected to the infrared cell (CaF_2 windows, 10-cm optical path) of a Bio-Rad Digilab FTS-45 FTIR spectrometer for the continuous monitoring of CO_2 via online absorption infrared spectrophotometry at 2349 cm^1. The gases contained in the (reactor + IR cell) assembly were recirculated (by means of a Schwartzer model 135 FZ micropump) every ~4 s. The reactor was immersed in a thermostat/cryostat (Neslab ULT-80) for temperature control. Photolyses involved irradiation of 1-mm-thick ice layers produced by freezing aqueous solutions (4 mL, previously sparged with 1 atm N_2 or O_2 at 293 K for 30 min) onto the reactor chamber walls. Ice layers were maintained at target temperatures for at least 2 hours prior to photolysis. Sample absorption and lamp emission spectra were recorded with a HP 8452A diode array spectrophotometer. Quantum yield (ϕ_{CO2}) measurements were based on the concerted photodecarboxylation of 10 mM BF (Aldrich 97%, used as received) reaction (2):

$$PhC(O)C(O)OH + h\nu \rightarrow PhC(O)H + CO_2 \quad (2)$$

as chemical actinometer [*Gorner and Khun*, 1999]. The concertedness of reaction (2) makes its course independent of the medium. Aqueous solutions of the radical scavenger 2,2,6,6-tetramethylpiperidin-1-oxyl (TEMPO, Aldrich 99%, purified by vacuum sublimation) were used in some experiments [*Guzmán et al.*, 2006b]. Control dark experiments confirmed that PA and BF are thermally stable under present reaction conditions.

[12] Organic product analysis were performed via high performance liquid chromatography (HPLC) at ambient temperature, using UV and electrospray ionization-mass spectrometric detection (Agilent 1100 series Model 1100 Series HPLC-MSD System), immediately after sample melting, as described in detail elsewhere [*Guzmán et al.*, 2006b].

3. Results and Discussion

3.1. CO_2 Photogeneration

[13] Figure 1 shows the CO_2 released during and after irradiation of frozen aqueous PA layers maintained at 248 K. Additional CO_2 is liberated upon melting the ice layers. The CO_2 values plotted in Figure 1 correspond to moles of CO_2 divided by the fluid volume of PA layers (4×10^{-3} L). We observed that CO_2 is immediately released and continues to evolve at nearly constant rates, upon irradiation at temperatures down to ~130 K. The latter is an upper limit imposed by instrumental sensitivity and corresponds to the temperature at which the sublimation pressure of solid CO_2 falls below detection limits [*Guzmán et al.*, 2006a]. Postirradiation CO_2 releases display single exponential growth kinetics: $CO_2(t) = CO_2(\infty) \times [1-\exp(-k_D t)]$, in isothermal experiments (Figure 2). Neither CO nor CH_4 were detected as gas-phase products in these experiments. Rate constants k_D (Figure 3) display Arrhenius temperature dependence:

$$\log\,(k_D/s^{-1}) = 1.08 - 1191/T \qquad (3)$$

between 227 and 269 K which corresponds to an apparent activation energy: $E_{a,D}$ = 22.8 kJ mol^{-1}, and A-factor: A_D = 12.1 s^{-1}.

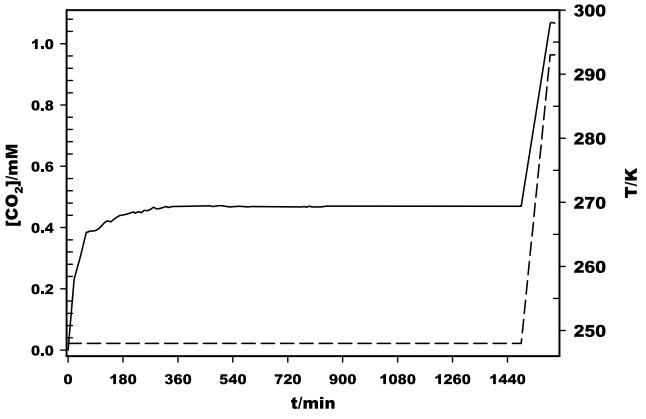

Figure 1. Solid trace (left axis), CO_2 released in the $\lambda \sim$ 313 nm photolysis of frozen, deareated aqueous pyruvic acid (4 mL, 100 mM, pH 1.0) solutions. CO_2 is released during the initial 60-min irradiation period and also in the post-illumination stage. Additional CO_2 is liberated upon thawing. Dashed trace (right axis), sample temperature.

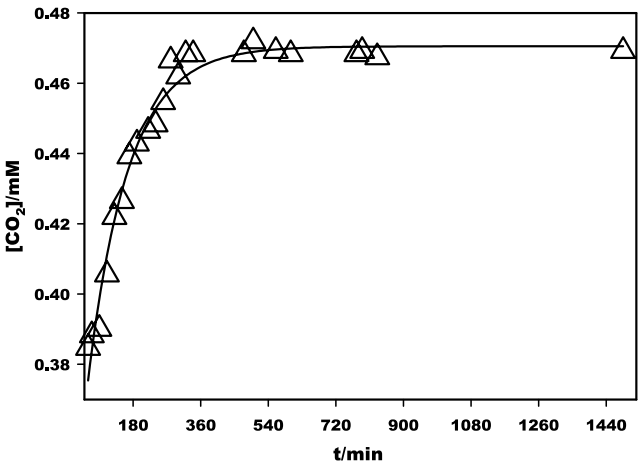

Figure 2. (Open triangle) A zoom of postirradiation CO_2 data from the experiment of Figure 1. Solid trace: $(CO_2) = A + B\,(1 - \exp(-k_D \times t)$; A = 0.304 mM; B= 0.167 mM; k_D = 9.307×10^{-3} min^{-1}.

[14] In a typical experiment, ~1.54 μmoles of CO_2 are released at the end of photolysis at 248 K. Additional CO_2 (up to a total of 1.87 μmoles of CO_2) is slowly released from irradiated frozen samples maintained at the same temperature. Further CO_2 evolves after thawing. Thus, only ~1% of the 400 μmoles of PA contained in the frozen layers is photolyzed in these experiments. About 50% of the photogenerated CO_2 ultimately escapes from frozen layers via a porous network open to the atmosphere, while the rest remains indefinitely trapped in the solid. The CO_2 amounts released after each stage are plotted as function of temperature in Figure 4. The apparent enthalpy change associated with overall CO_2 production, i.e., with the total CO_2 amounts recovered after melting, ΔH = (6.4 ± 1.6) kJ mol^{-1}, is suggestively similar to the enthalpy of ice melting: ΔH_M = 6.3 kJ mol^{-1}.

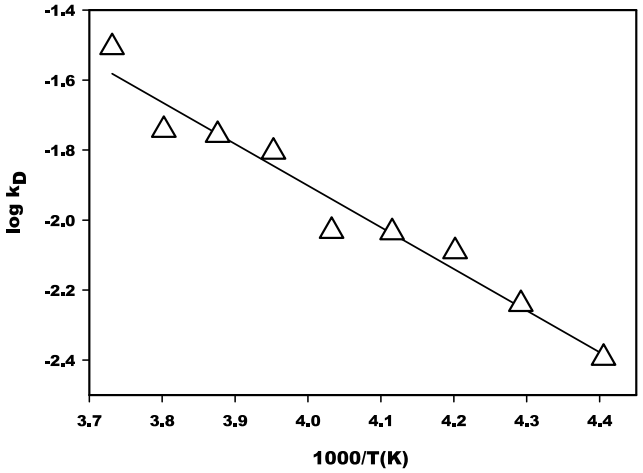

Figure 3. (Open triangle) Experimental first-order rate constants k_D for the release of CO_2 from previously photolyzed frozen pyruvic acid solutions. Solid trace: $\log\,(k_D/s^{-1}) = 1.08 - 1191/T$.

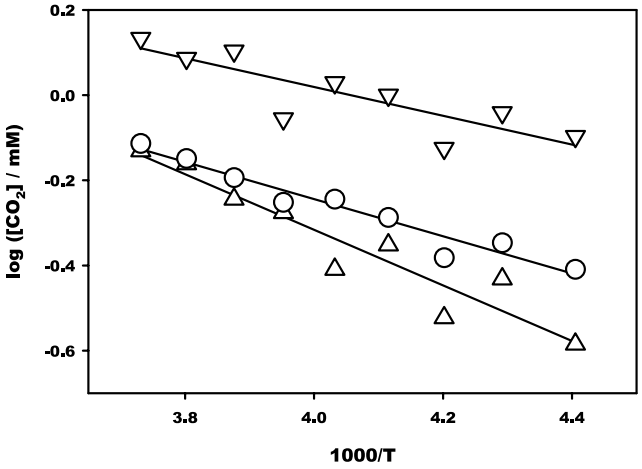

Figure 4. CO_2 released in the photolysis of frozen, deareated aqueous pyruvic acid (4 mL, 100 mM, pH 1.0) solutions as function of temperature. (Open triangle) Immediately after photolysis; (Open circle) before sample thawing; (Open inverted triangle) after sample thawing.

[15] Post-illumination CO_2 emissions from irradiated frozen PA solutions are not due to the slow desorption of preformed CO_2 but arise instead from an ongoing thermal reaction. This conclusion follows from the fact that post-illumination CO_2 emissions are absent in the photolysis of frozen BF solutions (Figure 5). The implication is that PA photolysis in ice proceeds, as in fluid solutions [*Guzmán et al.*, 2006b], via reactive intermediates and/or unstable species. In other words, unless further CO_2 were produced in the dark, the CO_2 photogenerated in ice cavities connected to the gas-phase is released fully and promptly (i.e., within a few seconds). The stepwise warming of pre-irradiated frozen PA samples further reveals that the CO_2 plateaus preceding each temperature jump in Figure 5 do not imply that the source of dark CO_2 has been exhausted, because additional CO_2 is chemically generated upon rising the temperature.

[16] Another mechanistic test is provided by the differential effect of radical scavengers on PA photolysis in ice and water. The photolysis of PA in water is known to be partially inhibited by radical scavengers [*Guzmán et al.*, 2006b], such as the persistent nitroxide 2,2,6,6-tetramethylpiperidin-1-oxyl (TEMPO) [*Beckwith et al.*, 1992; *Bowry and Ingold*, 1992; *Fischer*, 2001]. The fact that photochemical CO_2 production rates in aqueous PA solutions drop by a factor of two for [TEMPO] $\geq$1.7 mM [*Guzmán et al.*, 2006b] proves that half the CO_2 is produced in a fast pathway that cannot be intercepted by TEMPO, while the remainder arises from a slower process involving scavengeable radical intermediates. In contrast, the addition of TEMPO to prefrozen PA solutions has no effect whatsoever on CO_2 production rates during and after the photolysis of frozen PA solutions frozen under 1 atm N_2 (Figure 6). The efficiency of TEMPO as a radical scavenger is seemingly forfeited in frozen media by mobility restrictions. However, O_2(g) still behaves as a weak inhibitor both in fluid [*Gorner and Khun*, 1999] and frozen solutions; CO_2 production rates in the photolysis of frozen PA solutions performed under 1 atm O_2 are ~25% slower than under 1 atm N_2 at 253 K.

[17] Quantum yields for the overall production of CO_2 in reaction (1), ϕ_{CO_2}, in fluid and frozen aqueous PA solutions were determined from (1) measured rates of CO_2 evolution above aqueous solutions under continuous illumination and (2) the CO_2 amounts recovered after thawing frozen solutions that had been irradiated at constant temperature for specified periods of time, respectively. The effective absorption coefficients, ε_{eff}'s, of PA and BF in these experiments were evaluated from the convolution of their experimental absorption spectra in aqueous solution with the emission spectrum of the lamp. Since the extent of the

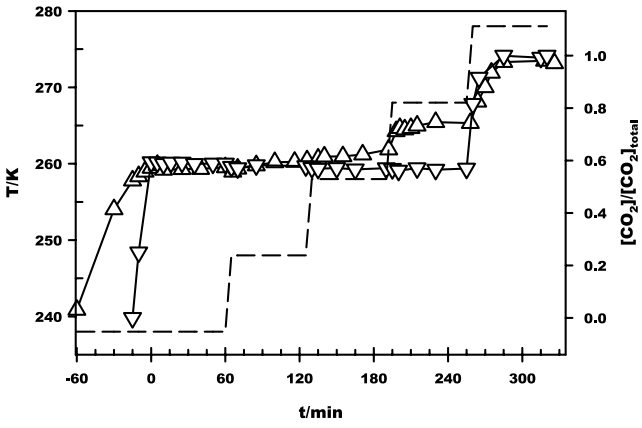

Figure 5. Symbols and solid traces (right axis), CO_2 fractions released immediately after (open triangle) 60 min photolysis of frozen, deareated aqueous pyruvic acid (4 mL, 100 mM, pH 1.0) and (open inverted triangle) 15 min photolysis of frozen, deareated aqueous benzoylformic acid (4 mL, 10 mM, pH 1.0). Dashed trace (left axis), sample temperature.

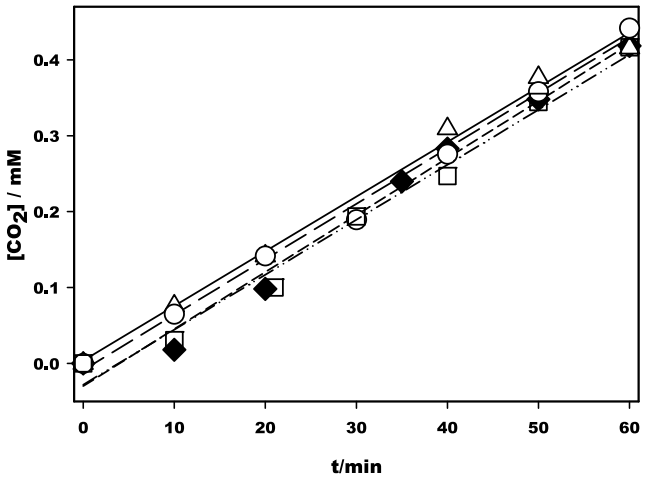

Figure 6. CO_2 released during irradiation of deareated aqueous pyruvic acid (4 mL, 100 mM, pH 1.0) doped with TEMPO frozen at 253 K. (Open triangle) without TEMPO; (solid diamond) (TEMPO) = 0.253 mM; (open circle) (TEMPO) = 0.994 mM; (open square) (TEMPO) = 2.403 mM. Although TEMPO partially inhibits PA photolysis in water in this concentration range [*Guzmán et al.*, 2006b], it has no effect on PA photolysis in ice.

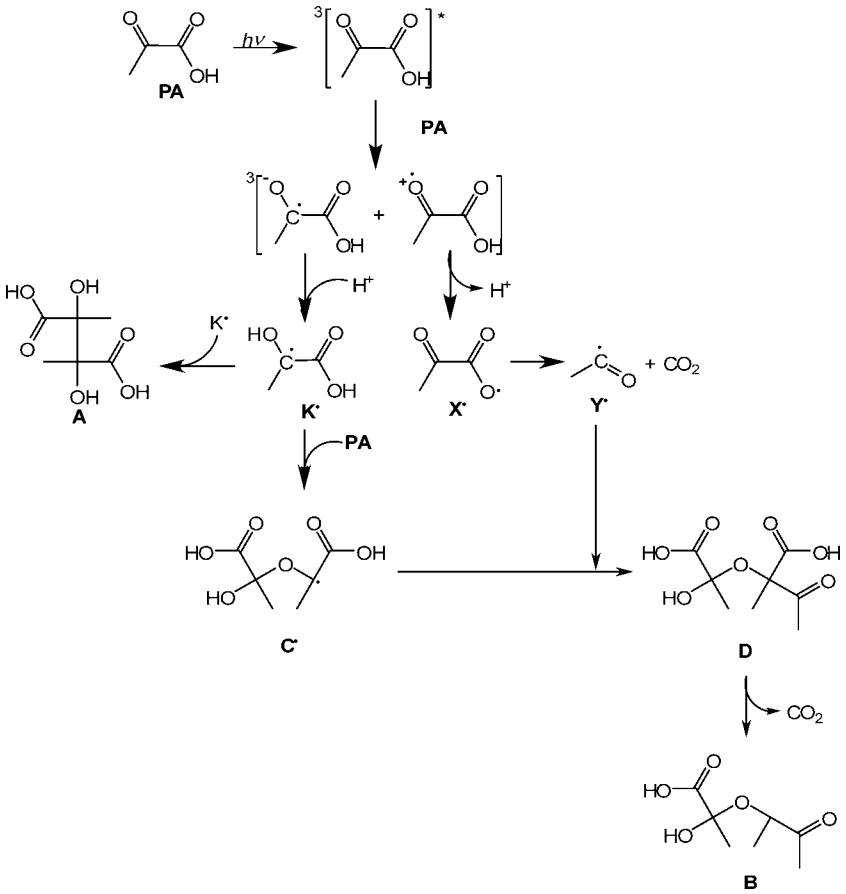

Scheme 1. Mechanism of pyruvic acid photolysis in ice.

partial hydration of keto-PA (*k*-PA), the actual chromophore, into transparent (above $\lambda > 300$ nm) 2,2-dihydroxypropanoic acid (*h*-PA) is an inverse function of temperature, the ε_{eff} of PA determined in water at 293 K was scaled down [ε_{eff} (<270 K) = 0.69 × ε_{eff} (293 K)] in frozen solutions according to the experimental ratios: [*h*-PA] / [*k*-PA] = 2.54 (293 K) and 4.10 (T < 270 K) measured by ^{1}H-NMR and reported elsewhere [*Buschmann et al.*, 1982; *Buschmann et al.*, 1980; *Guzmán et al.*, 2006c]. BF is barely hydrated under present conditions [*Fleury et al.*, 1977]. The assumption can be made that the quantum yield of CO_2 formation in the concerted photodecarboxylation of BF ($\phi_{CO_2,BF}$ = 0.39 at pH 3.0, 298 K)[*Gorner and Khun*, 1999; *Kuhn and Gorner*, 1988] does not change with physical state or temperature (c.f. with the intramolecular photoisomerization of 2-nitrobenzaldehyde) [*Dubowski et al.*, 2001]. The only reason for using PA and BF solutions of dissimilar concentrations is that they lead to comparable photolysis rates under present experimental conditions. Photolysis experiments in fluid and frozen BF or PA solutions led to: ϕ_{CO_2} = 0.78 ± 0.10 in water at 293 K (in excellent agreement with *Leermakers and Vesley* [1963], but a factor of two larger than our previously reported value) [*Guzmán et al.*, 2006b] and to the expression:

$$\log \phi_{CO_2} = (0.81 \pm 0.33) - (338 \pm 81)/T \qquad (4)$$

in frozen PA solutions down to 227 K. Equation (4) leads to an extrapolated value of ϕ_{CO_2} = 0.45 at 293 K, i.e., only ~40% smaller than in water (ϕ_{CO_2} = 0.78). These results confirm that the photodecarboxylation of PA, a typical ice core organic contaminant, proceeds with similar efficiency in ice and water.

3.2. Mechanism of Reaction

[18] The similar ϕ_{CO_2} values measured above and below the freezing point, and the fact that the organic products detected after thawing photolyzed frozen aqueous PA solutions are identical to those previously reported for the photolysis of fluid solutions, i.e., 2,3-dimethyl tartaric (A) and 2-(3-oxobutan-2-yloxy)-2-hydroxypropanoic acid (B) (Scheme 1) [*Guzmán et al.*, 2006b], indicate that PA photolysis follows the same course in fluid and frozen solutions. The initial chemical transformation results from electron transfer between the ^{3}PA* excited state and an adjacent PA molecule [*Guzmán et al.*, 2006a], followed by fast proton transfers that lead to the ketyl K· and carbonyloxyl X· radicals. While K· is stable and can engage in bimolecular reactions, the decarboxylation of the acetylcarbonyloxyl radical X· into acetyl radical Y·:

$$CH_3C(O)C(O)O\bullet \rightarrow CH_3C(O)\bullet + CO_2 \qquad (5)$$

occurs within a few vibrational periods even at low temperatures [*Abel et al.*, 2003; *Bockman et al.*, 1997]. The prompt release of CO_2 in the photolysis of frozen PA solutions down to at least ~130 K [*Guzmán et al.*, 2006a]

and the existence of a CO_2 fraction that cannot be scavenged by TEMPO in aqueous solution are both accounted for by reaction 5. Paramagnetic species disappear irreversibly from irradiated frozen aqueous PA solutions above ~190 K [*Guzmán et al.*, 2006a], i.e., all radicals ultimately recombine within nominally frozen matrices. While the direct recombination (K· + K· → A) leads to a 2,3-dimethyl tartaric acid, the addition of K· to PA yields yet another radical: K· + PA → C·. The recombination (C· + Y· → D) produces the C_8 β-oxocarboxylic acid D, whose slow decomposition gives rise to delayed CO_2 emissions.

[19] Scheme 1 comprises bimolecular events that entail large amplitude molecular motions, such as librations and center-of-mass translations, which can only take place in sufficiently fluid reaction media. The fact that ~2 mM TEMPO is not able to inhibit CO_2 emissions in 100 mM PA photolysis in ice, although it is effective in water, suggests that the allowed translational motions have a rather short range and only involve close molecular neighbors. The question of whether the requisite bimolecular reaction can be still invoked at the vastly smaller overall concentrations of organic matter present in natural ice cores deserves closer scrutiny (vide infra).

[20] The Arrhenius parameters: $E_{a,D} = 22.8$ kJ mol^{-1}, $A_D = 12.1$ s^{-1}, associated with k_D, the pseudo first-order rate constant for the decomposition of D in ice, are much smaller than those typical of the thermal decarboxylation of β-oxocarboxylic acids in aqueous solution ($E_a \sim 95$ kJ mol^{-1}, A-factor $\sim 10^{12}$–10^{13} s^{-1}) [*Guthrie*, 2002]. $A_D = 12.1$ s^{-1} represents an impossibly large negative activation entropy for an elementary reaction: $\Delta S \sim -230$ J K^{-1} mol^{-1} [*Andraos*, 2000; *Benson*, 1976]. Notice that $E_{a,D} = 22.8$ kJ mol^{-1} is nearly identical to the strength of the hydrogen bond in ice (~21 kJ mol^{-1}) [*Cotton and Wilkinson*, 1980; *Galwey et al.*, 2001]. However, as pointed out above, these parameters must be associated with a chemical reaction (the thermal decarboxylation of D) rather than with physical desorption of preformed CO_2. The production and release (from prephotolyzed frozen PA solutions) of limited amounts of CO_2 after discrete temperature jumps (Figure 4) are typical of the kinetic behavior displayed by intrinsically fast chemical reactions hindered by a cryogenic matrix [*Andraos*, 2000; *Spath and Raff*, 1992]. Since the decarboxylation of β-ketoacids is a highly concerted process involving four (or more) internal coordinates [*Guthrie*, 2002; *Huang et al.*, 1997], it is quite conceivable that a rigid ice matrix could block its decomposition. That the decomposition of D is actually controlled by the ice matrix is confirmed by the fact that the half-life, $\tau_D = 0.69 / k_D > 10$ min, in water at 293 K extrapolated from equation (3), should have led to measurably slow CO_2 emissions from thawed irradiated samples, at variance with observations.

3.3. Reaction Environments in Natural Versus Laboratory Ices

[21] An anonymous reviewer has argued that conclusions derived from present experiments are inapplicable to natural ices because (1) glacial ice is produced by the sintering of snow rather than by freezing aqueous solutions, (2) organic matter is likely to settle onto glacial ice carried by the atmospheric aerosol, and (3) the typical micromolar concentrations of individual organic acids in thawed natural ices [*Savarino and Legrand*, 1998] are orders of magnitude smaller than that used in this study.

[22] Natural and laboratory ices may differ in many ways, but what really matters in the present context are the molecular (nanoscopic) domains sensed by the solutes themselves rather than the macroscopic/mesoscopic ice textures and morphologies perceived by observers or revealed by microscopy at submicrometer resolution [*Baker et al.*, 2005; *Killawee et al.*, 1998]. Furthermore, the purported disparity in overall concentrations is rather incidental to ice photochemistry because it effectively refers to the disparity of solute concentrations measured in the fluids obtained by thawing natural versus laboratory ices, rather than to the local concentrations in the molecular domains where solutes reside and where photochemical processes actually take place in ice. In fact, in the presence of ice, the activity of water (and, hence, of the solute) in the unfrozen portion becomes an exclusive function of temperature, independent of the initial concentration of the aqueous solution [*Koop*, 2002]. In other words, when dilute solutions are cooled to (externally imposed) subfreezing temperatures, they freeze out more water than concentrated solutions (the lever rule [*Reisman*, 1970]), and vice versa, to comply with this thermodynamic constraint [*Koop*, 2002]. Intensive variables, such as solute concentration in the unfrozen portion, depend on temperature and pressure. Only the volume fraction of the unfrozen portion is proportional to total amount of solute in the sample. We recently confirmed that the activity of water, as probed by magic angle spinning ^{1}H-NMR measurements of the "gem"-diol PA/keto PA ratio in frozen aqueous PA solutions, becomes independent of the initial concentrations of aqueous PA solutions cooled below ~250 K [*Guzmán et al.*, 2006c]. The contention that solute concentration in the unfrozen portion somehow depends on the initial concentration of the aqueous solution is, therefore, untenable. Practical considerations (such as duration of experiments × detection limits) dictate the use of larger solute concentrations in laboratory experiments.

[23] Size restrictions allow only small species to be incorporated as substitutional impurities into the ice phase. Most organic and inorganic solutes [*Killawee et al.*, 1998] (particularly the macromolecular humic-like substances relevant to this discussion) will be segregated from the ice phase into highly concentrated fluid or glassy media upon freezing [*Boxe et al.*, 2005; *Boxe et al.*, 2006; *Boxe et al.*, 2003; *Heger et al.*, 2005]. Recently, it was found that by slowly freezing 0.1 μM aqueous methylene blue (MW = 374 Da, a fair surrogate of dissolved natural organic matter) solutions, the solute is concentrated by at least 6 orders of magnitude in the unfrozen portion remaining at 243 K [*Heger et al.*, 2005]. In a related study, we found that the second order hydrolysis of the NO_2 produced in situ during the photolysis of nitrate in ice, reaction 6:

$$2NO_2(g) + H_2O(l) \rightleftarrows NO_3^-(aq) + NO_2^-(aq) + 2\ H^+(aq) \quad (6)$$

is still significant in frozen micromolar nitrate solutions [*Boxe et al.*, 2006]. Therefore most molecular ice impurities are generally expected to be located in low-dimensional fluid phases at concentrations that are vastly larger than

those measured in thawed ice core samples. The acidities experienced in ice at the molecular level are also remotely related to those of the thawed samples and are determined by specific ion combinations [*Heger et al.*, 2006; *Robinson et al.*, 2006].

[24] Still, as previously pointed out, most solutes probably land on surface snow (and become embedded in glacial ice after several decades) effectively encapsulated in prefrozen atmospheric aerosol microdroplets. If these microbeads were to remain intact, solute molecules would not be incorporated as isolated impurities in the ice matrix by this mechanism either, because typical 1-μm radii aqueous droplets consist of $\sim 2 \times 10^{11}$ H_2O molecules or $\sim 2 \times 10^5$ molecules of a solute present at ppm levels (PA > 18 ppm in urban aerosol at 50% relative humidity [*Guzmán et al.*, 2006b; *Kawamura et al.*, 2005; *Kawamura and Yasui*, 2005]). Furthermore many organic solutes are expected to crowd during freezing, driven by intermolecular interactions such as hydrophobic forces in the case of nonpolar species or hydrogen bonding in the case of PA dimers. At the modest droplet cooling rates prevailing in the atmosphere ($\sim$1 K min^{-1} [*Haag et al.*, 2003] versus the 10^5 K min^{-1} rates required to hyperquench water into amorphous glassy water [*Bednarek et al.*, 1996]) departures from equilibrium solute distributions are expected to be minor [*Haag et al.*, 2003; *Stuart and Jacobson*, 2006] and relax during the subsequent firnification process. Notice that the extended hydraulic networks filled by concentrated solutions detected in glacial ice [*Nye*, 1989] could only be created from a material consisting of randomly distributed concentrated spots (such as that produced by the deposition of frozen aerosol beads on ground snow) via strain-induced melting and recrystallization. The existence of quasi-fluid aqueous domains of nanoscopic dimensions containing significant numbers of solute molecules in close proximity, as strictly required by the mechanism of Scheme 1, seems ensured, therefore, under natural and laboratory conditions.

3.4. Photochemical Origin of CO and CO_2 Ice Core Records Irregularities

[25] It has been generally assumed that given the prevalent low temperatures [*Price et al.*, 2002], and the fact that sunlight is completely blocked within a few meters below the surface by the highly reflective snow/firn cover) [*Belzile et al.*, 2000; *Gerland et al.*, 1999; *Glendinning and Morris*, 1999; *Phillips and Simpson*, 2005] species immobilized in deep ice core layers, i.e., below the firn line, will indefinitely retain their chemical identity. Thus the fact that CO and CO_2 levels in Greenland ice core records dating from the last two millenia exceed those in contemporaneous Antarctic records by up to 130 ppbv and 20 ppmv (i.e., well beyond their experimental uncertainties), respectively [*Haan and Raynaud*, 1998; *Tschumi and Stauffer*, 2000], is an unexpected finding that seems to undermine the archival value of polar records and demands a plausible explanation. The anomalies are not restricted to interhemispheric differences because CO_2 concentrations in Siple Dome, Antarctica, from certain periods of the Holocene are also larger than in other Antarctic sites by up to 20 ppmv [*Ahn et al.*, 2004]. The fact that outliers appear as sharp spikes superimposed on otherwise normal time series rules out analytical errors and militates against diffusional processes within the ice matrix. At stake is the issue of whether these anomalies are exceptional and, if so, why.

[26] Several hypothesis have been advanced to account for the abnormal records [*Monnin et al.*, 2001]. "The sudden occurrence of high CO concentrations at about 155 m depths suggests the presence of organic species that are able to produce carbon monoxide" [*Haan and Raynaud*, 1998]. "The most probable explanation for CO_2 peak values in thin core sections representing only a few annual layers, or even less than an annual layer, specially in Greenland ice, is production of CO_2 by chemical reactions between impurities in the cold ice" [*Tschumi and Stauffer*, 2000]. Possible CO_2 production mechanism include [*Ahn et al.*, 2004] (1) acidification of carbonates [*Anklin et al.*, 1995; *Barnola et al.*, 1995; *Delmas*, 1993], (2) chemical [*Tschumi and Stauffer*, 2000], or (3) biological oxidation of organic compounds [*Campen et al.*, 2003; *Mader et al.*, 2006; *Price and Sowers*, 2004].

[27] Both polar ice caps are known to be contaminated by organic material or continental or marine origin [*Desideri et al.*, 1998; *Gayley and Ram*, 1985; *Kawamura et al.*, 1995], but Greenland ice cores are conspicuously spoiled by the scavenging of organic gases and deposition of the organic aerosol released by major, epochal boreal forest fires [*Domine and Shepson*, 2002; *Kawamura et al.*, 1995; *Kawamura et al.*, 2001; *Savarino and Legrand*, 1998]. Full speciation of the organic matter present in polar ice remains a daunting analytical challenge [*Grannas et al.*, 2006], but it is generally agreed that organic contaminants largely consist of humic-like substances, such as those globally present in natural waters, the simpler products of their solar photodegradation [*Gao and Zepp*, 1998; *Miller and Zepp*, 1995; *Moran and Zepp*, 1997; *Opsahl and Zepp*, 2001; *Valentine and Zepp*, 1993], as well as the products of the photooxidation of atmospheric organic substances, such as dicarboxylic, α-oxocarboxylic and ω-oxocarboxylic acids, and α-dicarbonyl species [*Kawamura et al.*, 2005; *Kawamura et al.*, 1996; *Kawamura et al.*, 2001; *Wang et al.*, 2006]. Pyruvic acid, 2-oxopropanoic acid, is a ubiquitous representative of these species.

[28] The photochemical degradation of dissolved organic matter in the atmosphere, surface waters, and snow [*Grannas et al.*, 2004; *Osburn et al.*, 2001] yields CO [*Mopper et al.*, 1991; *Schade et al.*, 1999; *Valentine and Zepp*, 1993] and CO_2 [*Johannessen and Miller*, 2001]. Quantum yields of CO_2 and CO photoproduction, which depend somewhat on the origin of dissolved organic matter, decrease exponentially at longer wavelengths [*Johannessen and Miller*, 2001; *Valentine and Zepp*, 1993]. Relative yields vary in the range $20 \leq \phi_{CO_2} / \phi_{CO} \leq 50$. The possibility that photochemical processes similar to those occurring in surface waters could occur in deep ice, and therefore contaminate paleorecords, has been implicitly discounted because of the high reflectivity of the snow cover to ultraviolet light, the lack of a conceivable in situ source of actinic radiation and the absence of documented examples of photoinduced decarboxylations/decarbonylations in frozen aqueous media. Still, "even the highly improbable must be considered over the long timescales involved in ice core chemistry. Organic acids and other C-containing species present in sufficient quantities have the potential

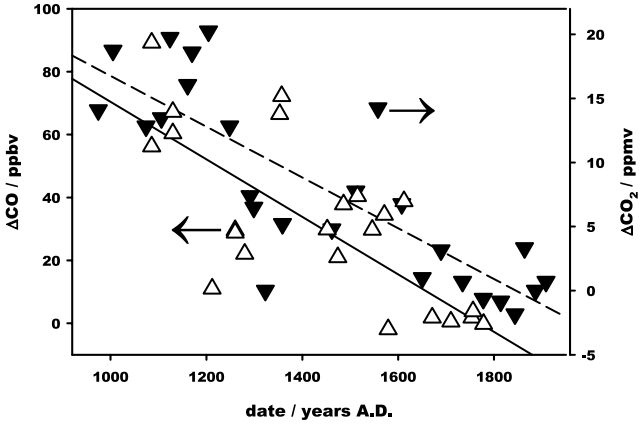

Figure 7. (Solid inverted triangle) Differences between CO_2 (ppmv) readings from Greenland (Eurocore, GRIP) and Antarctic (South Pole, D47, D57) ice core records (right axis) versus date (*Anklin et al.*, 1995). (Open triangle) Differences between CO (ppbv) readings from Greenland (Eurocore, GRIP) relative to the constant value (89 ppbv) for the period 1640–1870 AD, (left axis) versus date [*Haan and Raynaud*, 1998].

to influence CO and CO_2, if a reasonable mechanism were proposed'' [*Wolff*, 1996].

[29] We have recently proposed and quantified the likelihood that the dissolved organic matter trapped in ice cores could be photodegraded by the ultraviolet Çerenkov radiation generated by cosmic muons [*Colussi and Hoffmann*, 2003]. By assuming that the quantum yields of decarbonylation of dissolved organic matter were similar in ice and water, the timing and magnitude of the CO anomalies in Greenland versus coeval Antarctic ice core bubbles dating from the Middle Ages could be plausibly correlated with the occurrence of boreal fires [*Savarino and Legrand*, 1998]. This analysis revealed that significant photochemistry could be induced in deep ice by Çerenkov radiation over geological periods. Despite the small local photon production rates, the exceptional transparency of pristine glacial ice between 200 and 500 nm [*Askebjer et al.*, 1997a; *Askebjer et al.*, 1997b] allows chromophoric point impurities, such as those created by sporadic contamination from dissolved organic matter, to be photochemically processed not only by locally generated photons but also from those created elsewhere and collected onto the absorbing layer after diffusing through the ice matrix. A strongly absorbing sink effectively acts as an antenna whose collection efficiency is proportional to the ratio of the thickness of the pristine layer to the effective thickness of the layer containing the organic chromophore. This ratio depends, in general, on dust levels in the ice, as well as on chromophore concentration and absorptivity [*Colussi and Hoffmann*, 2003].

[30] A comparison between CO [*Haan and Raynaud*, 1998] and CO_2 excesses [*Anklin et al.*, 1995] in Eurocore sites versus Antarctic profiles as function of gas age (Figure 7) shows that they not only follow similar trends, but the ratio of the slopes: $S_{CO_2} / S_{CO} \sim 200$, falls in the range of the ratio of quantum yields, ϕ_{CO_2} / ϕ_{CO}, for the production of dissolved inorganic carbon (that should appear as CO_2 in ice) and CO in the solar photolysis of dissolved organic matter in natural waters [*Gao and Zepp*, 1998; *Johannessen and Miller*, 2001; *Kieber et al.*, 1989; *Mopper et al.*, 1991; *Moran and Zepp*, 1997; *Opsahl and Zepp*, 2001; *Valentine and Zepp*, 1993; *Zuo and Jones*, 1996]. A more stringent comparison should, of course, involve ϕ's for the photolysis of dissolved organic matter in ice by (Çerenkov) radiation in the range $200 < \lambda/\text{nm} < 400$, rather than in water under solar ($\lambda > 300$ nm) radiation. Notice that increasing deviations in older ice deposits support continuous photochemistry under an in situ incessant radiation source, such as that provided by Çerenkov radiation, but rules out photochemistry in the upper ice layers for the limited periods during which they are exposed to sunlight. Present results and analysis, together with the data of Figure 7, represent strong evidence that the in situ photochemistry of organic ice contaminants is a physically and chemically plausible mechanism that could account, in principle, for the observed ice core records anomalies.

[31] **Acknowledgments.** This work was financed by NSF grant ATM-0228140. Nathan Dalleska (Caltech Environmental Analysis Center) provided valuable technical assistance.

References

Abel, B., J. Assmann, M. Buback, C. Grimm, M. Kling, S. Schmatz, J. Schroeder, and T. Witte (2003), Ultrafast decarboxylation of carbonyloxy radicals: Influence of molecular structure, *J. Phys. Chem. A*, *107*, 9499–9510.

Ahn, J., M. Wahlen, B. L. Deck, E. J. Brook, P. A. Mayewski, K. C. Taylor, and J. W. C. White (2004), A record of atmospheric CO_2 during the last 40,000 years from the Siple Dome, Antarctica ice core, *J. Geophys. Res. Atmos.*, *109*, D13305.

Andraos, J. (2000), Bimolecular kinetics at low temperatures using FTIR matrix isolation spectroscopy: Some caveats. Thermokinetic parameters for the reaction pf fulvenones with pyridine in pyridine Matrixes, *J. Phys. Chem. A*, *104*, 1532–1543.

Andres, E., et al. (2001), Observation of high-energy neutrinos using Cerenkov detectors embedded deep in Antarctic ice, *Nature*, *410*(6827), 441–443.

Anklin, M., J. M. Barnola, J. Schwander, B. Stauffer, and D. Raynaud (1995), Processes affecting the CO_2 concentrations measured in Greenland Ice, *Tellus*, *47 B*(4), 461–470.

Askebjer, P., et al. (1997a), Optical properties of deep ice at the South Pole: Absorption, *Appl. Opt.*, *36*(18), 4168–4180.

Askebjer, P., et al. (1997b), UV and optical light transmission properties in deep ice at the South Pole, *Geophys. Res. Lett.*, *24*(11), 1355–1358.

Baker, I., D. Iliescu, R. Obbard, H. Chang, B. Bostick, and C. P. Daghlian (2005), Microstructural characterization of ice cores, *Ann. Glaciol.*, *42*, 441–444.

Barnola, J. M., M. Anklin, J. Porcheron, D. Raynaud, J. Schwander, and B. Stauffer (1995), CO_2 evolution during the last millennium as recorded by Antarctic and Greenland Ice, *Tellus*, *47 B*, 264–272.

Beckwith, A. L. J., V. W. Bowry, and K. U. Ingold (1992), Kinetics of nitroxide radical trapping: 1. Solvent effects, *J. Am. Chem. Soc.*, *114*, 4983–4992.

Bednarek, J., A. Plonka, A. Hallbrucker, E. Mayer, and M. C. R. Symons (1996), Hydroperoxyl radical generation by gamma-irradiation of glassy water at 77 K, *J. Am. Chem. Soc.*, *118*, 9387–9390.

Belzile, C., S. C. Johannessen, M. Gosselin, S. Demers, and W. L. Miller (2000), Ultraviolet attenuation by dissolved and particulate constituents of first-year ice during late spring in an Arctic polynya, *Limnol. Oceanogr.*, *45*, 1265–1273.

Benson, S. W. (1976), *Thermochemical Kinetics*, John Wiley, Hoboken, N. J. New York.

Bockman, T. M., S. M. Hubig, and J. K. Kochi (1997), Direct observation of ultrafast decarboxylation of acyloxy radicals via photoinduced electron transfer in carboxylate ion pairs, *J. Org. Chem.*, *62*, 2210–2221.

Boucot, A. J., and J. Gray (2001), A critique of Phanerozoic climatic models involving changes in the CO_2 content of the atmosphere, *Earth-Sci. Rev.*, *56*, 1–159.

Bowry, V. W., and K. U. Ingold (1992), Kinetics of nitroxide radical trapping: 2. Structural effects, *J. Am. Chem. Soc.*, *114*, 4992–4996.

Boxe, C. S., A. J. Colussi, M. R. Hoffmann, D. Tan, J. Mastromarino, A. T. Case, S. T. Sandholm, and D. D. Davis (2003), Multiscale ice

fluidity in NO_x photodesorption from frozen nitrate solutions, *J. Phys. Chem. A*, *107*, 11409–11413.
Boxe, C. S., A. J. Colussi, M. R. Hoffmann, J. G. Murphy, P. J. Wooldridge, T. H. Bertram, and R. C. Cohen (2005), Photochemical production and release of gaseous NO_2 from nitrate-doped water ice, *J. Phys. Chem. A*, *109*, 8520–8525.
Boxe, C. S., A. J. Colussi, M. R. Hoffmann, I. M. Perez, J. G. Murphy, and R. C. Cohen (2006), Kinetics of NO and NO_2 evolution from illuminated frozen nitrate solutions, *J. Phys. Chem. A*, *110*, 3578–3583.
Brook, E. J. (2005), Tiny bubbles tell all, *Science*, *310*, 1285–1287.
Budac, D., and P. Wan (1992), Photodecarboxylation: mechanism and synthetic utility, *J. Photochem. Photobiol. A: Chem.*, *67*, 135–166.
Burden, D. L., and G. M. Hieftje (1998), Çerenkov radiation as a UV and visible light source for time-resolved fluorescence, *Anal. Chem.*, *70*(16), 3426–3433.
Buschmann, H. J., H. H. Fuldner, and W. Knoche (1980), The reversible hydration of carbonyl compounds in aqueous solution: Part I. The keto/gem-diol equilibrium, *Ber. Bunseges. Phys. Chem.*, *84*, 41–44.
Buschmann, H. J., E. Dutkiewicz, and W. Knoche (1982), The reversible hydration of carbonyl compounds in aqueous solutions. Part II: The kinetics of the keto-gem-diol transition, *Ber. Bunseges. Phys. Chem.*, *86*, 129–134.
Calace, N., B. M. Petronio, R. Cini, A. M. Stortini, B. Pampaloni, and R. Udisti (2001), Humic marine matter and insoluble materials in Antarctic snow, *Int. J. Environ. Anal. Chem.*, *79*(4), 331–348.
Campen, R. K., T. Sowers, and R. B. Alley (2003), Evidence of microbial consortia metabolyzing within a low-latitude mountain glacier, *Geology*, *31*, 231–234.
Closs, G. L., and R. J. Miller (1978), Photoreduction and photodecarboxylation of pyruvic acid. Applications of CINDP to mechanistic photochemistry, *J. Am. Chem. Soc.*, *100*, 3483–3494.
Colussi, A. J., and M. R. Hoffmann (2003), In situ photolysis of deep ice core contaminants by Cerenkov radiation of cosmic origin, *Geophys. Res. Lett.*, *30*(4), 1195, doi:10.1029/2002GL016112.
Cotton, F. A., and G. Wilkinson (1980), *Advanced Inorganic Chemistry*, John Wiley, Hoboken, N. J.
Cowen, D. F., et al. (2001), Recent results from AMANDA, *Int. J. Mod. Phys. A*, *16*(Suppl. 1C), 1013–1015.
Delmas, R. J. (1993), A natural artefact in Greenland ice-core CO_2 measurements, *Tellus*, *45 B*(4), 391–396.
Desideri, P. G., L. Lepri, R. Udisti, L. Checchini, M. Del Bubba, R. Cini, and A. M. Stortini (1998), Analysis of organic compounds in Antarctic snow and their origin, *Int. J. Environ. Anal. Chem.*, *71*(3–4), 331–351.
Do, J. S., and C. P. Chen (1994), In-situ oxidative degradation of formaldehyde with hydrogen peroxide electrogenerated on modified graphites, *J. Appl. Electrochem.*, *24*, 936–942.
Domine, F., and P. B. Shepson (2002), Air-snow interactions and atmospheric chemistry, *Science*, *297*(5586), 1506–1510.
Dubowski, Y., A. J. Colussi, and M. R. Hoffmann (2001), Nitrogen dioxide release in the 302 nm band photolysis of spray-frozen aqueous nitrate solutions. Atmospheric implications, *J. Phys. Chem. A*, *105*(20), 4928–4932.
EPICA (2004), Eight glacial cycles from an Antarctic ice core, *Nature*, *429*, 623–628.
Fischer, H. (2001), The persistent radical effect: A principle for selective radical reactions and living radical polymerizations, *Chem. Rev.*, *101*, 3581–3610.
Fischer, H., M. Wahlen, J. Smith, D. Mastroianni, and B. L. Deck (1999), Ice core records of atmospheric CO_2 around the last three glacial terminations, *Science*, *283*, 1712–1714.
Fleury, M. B., J. Moiroux, D. Fleury, and J. C. Dufresne (1977), Consequences of acceptor effects on polarization of oxo and imine bonds in acyl and R–CO–COOH compounds: Part 3. Acid-base equilibria antecedent to reduction of α-ketoacids at DME, *J. Electroanal. Chem.*, *81*, 365–376.
Galwey, A. K., D. B. Sheen, and J. N. Sherwood (2001), Should the melting of ice be represented as a solid state reaction?, *Thermochim. Acta*, *375*, 161–167.
Gao, H. Z., and R. G. Zepp (1998), Factors influencing photoreactions of dissolved organic matter in a coastal river of the southeastern United States, *Environ. Sci. Technol.*, *32*(19), 2940–2946.
Gayley, R. I., and M. Ram (1985), Atmospheric dust in polar ice and the background aerosol, *J. Geophys. Res.*, *90*, 12,921–12,925.
Gerland, S., J. G. Winther, J. B. Orbaek, G. E. Liston, N. A. Oritsland, A. Blanco, and B. Ivanov (1999), Physical and optical properties of snow covering Arctic tundra on Svalbard, *Hydrol. Process.*, *13*(14–15), 2331–2343.
Glendinning, J. H. G., and E. M. Morris (1999), Incorporation of spectral and directional radiative transfer in a snow model, *Hydrol. Process.*, *13*, 1761–1772.
Gorner, H., and H. J. Khun (1999), Photodecarboxylation of phenylglyoxylic acid: Influence of para-substituents on the triplet state properties, *J. Chem. Soc., Perkin Trans.*, *2*(12), 2671–2680.
Grannas, A. M., et al. (2002), A study of photochemical and physical processes affecting carbonyl compounds in the Arctic atmospheric boundary layer, *Atmos. Environ.*, *36*(15–16), 2733–2742.
Grannas, A. M., P. B. Shepson, and T. R. Filley (2004), Photochemistry and nature of organic matter in Arctic and Antarctic snow, *Global Biogeochem. Cycles*, *18*(1), GB1006, doi:10.1029/2003GB002133.
Grannas, A. M., W. C. Hockaday, P. G. Hatcher, L. G. Thompson, and E. Mosley-Thompson (2006), New revelations on the nature of organic matter in ice cores, *J. Geophys. Res.*, *111*, D04304, doi:10.1029/2005JD006251.
Guthrie, J. P. (2002), Uncatalyzed and amine catalyzed decarboxylation of acetolactic acid: An examination in terms of barrier theory, *Bioorg. Chem.*, *30*, 32–52.
Guzmán, M. I., A. J. Colussi, and M. R. Hoffmann (2006a), Photogeneration of distant radical pairs in aqueous pyruvic acid glasses, *J. Phys. Chem. A*, *110*, 931–935.
Guzmán, M. I., A. J. Colussi, and M. R. Hoffmann (2006b), Photoinduced oligomerization of aqueous pyruvic acid, *J. Phys. Chem. A*, *110*, 3619–3626.
Guzmán, M. I., L. Hildebrandt, A. J. Colussi, and M. R. Hoffmann (2006c), Cooperative hydration of pyruvic acid in ice, *J. Am. Chem. Soc.*, *128*, 10,621–10,624.
Haag, W., B. Karcher, S. Schaefers, O. Stetzer, O. Mohler, U. Schurath, M. Kramer, and C. Schiller (2003), Numerical simulations of homogeneous freezing processes in the aerosol chamber AIDA, *Atmos. Chem. Phys.*, *3*, 195–210.
Haan, D., and D. Raynaud (1998), Ice core record of CO variations during the last two millennia: Atmospheric implications and chemical interactions within the Greenland ice, *Tellus*, *50 B*, 253–262.
Haan, D., P. Martinerie, and D. Raynaud (1996), Ice core data of atmospheric carbon monoxide over Antarctica and Greenland during the last 200 years, *Geophys. Res. Lett.*, *23*, 2235–2238.
Heger, D., J. Jirkovsky, and P. Klan (2005), Aggregation of methylene blue in frozen aqueous solutions studied by absorption spectroscopy, *J. Phys. Chem. A*, *109*, 6702–6709.
Heger, D., J. Klanova, and P. Klan (2006), Enhanced protonation of cresol red in acidic aqueous solutions caused by freezing, *J. Phys. Chem. B*, *110*, 1277–1287.
Huang, C. L., C. C. Wu, and M. H. Lien (1997), Ab initio studies of decarboxylations of β-ketocarboxylic acids XCOCHCOOH (X = H, OH, CH_3), *J. Phys. Chem. A*, *101*, 7867–7873.
Hutterli, M. A., J. R. McConnell, R. C. Bales, and R. W. Stewart (2003), Sensitivity of hydrogen peroxide (H_2O_2) and formaldehyde (HCHO) preservation in snow to changing environmental conditions: Implications for ice core records, *J. Geophys. Res.*, *108*(D1), 4023, doi:10.1029/2002JD002528.
Johannessen, S. C., and W. L. Miller (2001), Quantum yield for the photochemical production of dissolved inorganic carbon in seawater, *Mar. Chem.*, *76*(4), 271–283.
Kawamura, K., and O. Yasui (2005), Diurnal changes in the distribution of dicarboxylic acids, ketocarboxylic acids and dicarbonyls in the urban Tokyo atmosphere, *Atmos. Environ.*, *39*, 1945–1960.
Kawamura, K., H. Kasukabe, O. Yasui, and L. A. Barrie (1995), Production of dicarboxylic acid in the arctic atmosphere at polar sunrise, *Geophys. Res. Lett.*, *22*, 1253–1256.
Kawamura, K., H. Kasukabe, and L. A. Barrie (1996), Source and reaction pathways of dicarboxylic acids, ketoacids and dicarbonyls in Arctic aerosols: One year of observations, *Atmos. Environ.*, *30*, 1709–1722.
Kawamura, K., K. Yokoyama, Y. Fujii, and O. Watanabe (2001), A Greenland ice core record of low molecular weight dicarboxylic acids, ketocarboxylic acids, and alpha-dicarbonyls: A trend from Little Ice Age to the present (1540 to 1989 AD), *J. Geophys. Res.*, *106*(D1), 1331–1345.
Kawamura, K., T. Nakazawa, S. Aoki, S. Sugawara, Y. Fujii, and O. Watanabe (2003), Atmospheric CO_2 variations over the last three glacial-interglacial climatic cycles deduced from the Dome Fuji deep ice core, Antarctica using a wet extraction technique, *Tellus*, *55 B*, 126–137.
Kawamura, K., Y. Imai, and L. A. Barrie (2005), Photochemical production and loss of organic acids in high Arctic aerosols during long-range transport and polar sunrise ozone depletion events, *Atmos. Environ.*, *39*(4), 599–614.
Kieber, D. J., J. McDaniel, and K. Mopper (1989), Photochemical source of biological substrates in sea-water—Implications for carbon cycling, *Nature*, *341*, 637–639.
Killawee, J. A., I. J. Fairchild, J. L. Tison, L. Janssens, and R. Lorrain (1998), Segregation of solutes and gases in experimental freezing of dilute solutions: Implications for natural glacial systems, *Geochim. Cosmochim. Acta*, *62*, 3637–3655.

Koop, T. (2002), The water activity of aqueous solutions in equilibrium with ice, *Bull. Chem. Soc. Jpn.*, *75*, 2587–2588.

Kuhn, H. J., and H. Gorner (1988), Triplet state and photodecarboxylation of phenylglyoxylic acid in the presence of water, *J. Phys. Chem.*, *92*, 6208–6219.

Landais, A., et al. (2006), Firn-air $\delta^{15}N$ in modern polar sites and glacial-interglacial ice: A model-data mismatch during glacial periods in Antarctica?, *Quat. Sci. Rev.*, *25*, 49–62.

Leermakers, P. A., and G. F. Vesley (1963), The photochemistry of alpha-keto acids and alpha-keto esters. I. Photolysis of pyruvic acid and benzoylformic acid, *J. Am. Chem. Soc.*, *85*, 3776–3779.

Mader, H. M., J. L. Wadham, E. W. Wolff, and R. J. Parkes (2006), Subsurface ice as a microbial habitat, *Geology*, *34*, 169–172.

McElroy, W. J., and S. J. Waygood (1991), Oxidation of formaldehyde by the hydroxyl radical in aqueous-solution, *J. Chem. Soc. Faraday Trans.*, *87*, 1513–1521.

Miller, W. M., and R. G. Zepp (1995), Photochemical production of dissolved inorganic carbon from terrestrial organic-matter. Significance to the oceanic organic-carbon cycle, *Geophys. Res. Lett.*, *22*, 417–420.

Monnin, E., A. Indermuhle, A. Dallenbach, J. Fluckiger, B. Stauffer, T. F.Stocker, D. Raynaud, and J. M. Barnola (2001), Atmospheric CO_2 concentrations over the last glacial termination, *Science*, *291*, 112–114.

Mopper, K., X. Zhou, R. J. Kieber, R. G. Sikorski, and R. D. Jones (1991), Photochemical degradation of dissolved organic carbon and its impact on the oceanic carbon cycle, *Nature*, *353*, 60–62.

Moran, M. A., and R. G. Zepp (1997), Role of photoreactions in the formation of biologically labile compounds from dissolved organic matter, *Limnol. Oceanogr.*, *42*(6), 1307–1316.

Mudelsee, M. (2001), The phase relations among atmospheric CO_2 content, temperature and global ice volume over the past 420 ka, *Quat. Sci. Rev.*, *20*, 583–589.

North Greenland Ice Core Project Memebers (2004), High-resolution record of Northern Hemisphere climate extending into the last interglacial period, *Nature*, *431*(7005), 147–151.

Nye, J. F. (1989), The geometry of water veins and nodes in polycrystalline ice, *J. Glaciol.*, *35*, 17.

Opsahl, S. P., and R. G. Zepp (2001), Photochemically-induced alteration of stable carbon isotope ratios (delta C-13) in terrigenous dissolved organic carbon, *Geophys. Res. Lett.*, *28*, 2417–2420.

Osburn, C. L., D. P. Morris, K. A. Thorn, and R. E. Moeller (2001), Chemical and optical changes in freshwater dissolved organic matter exposed to solar radiation, *Biogeochemistry*, *54*(3), 251–278.

Pearson, P. N., and M. R. Palmer (2000), Atmospheric carbon dioxide concentrations over the past 60 million years, *Nature*, *406*, 695–699.

Phillips, G. J., and W. R. Simpson (2005), Verification of snowpack radiation transfer models using actinometry, *J. Geophys. Res.*, *110*, D08306, doi:10.1029/2004JD005552.

Price, P. B., and T. Sowers (2004), Temperature dependence of metabolic rates for microbial growth, maintenance, and survival, *Proc. Natl. Acad. Sci. U. S. A.*, *101*, 4631–4636.

Price, P. B., O. V. Nagornov, R. Bay, D. Chirkin, Y. D. He, P. Miocinovic, A. Richards, K. Woschnagg, B. Koci, and V. Zagorodnov (2002), Temperature profile for glacial ice at the South Pole: Implications for life in a nearby subglacial lake, *Proc. Natl. Acad. Sci. U. S. A.*, *99*, 7844–7847.

Reisman, A. (1970), *Phase Equilibria: Basic Principles, Applications, Experimental Techniques*, Elsevier, New York.

Robinson, C., C. S. Boxe, M. I. Guzmán, A. J. Colussi, and M. R. Hoffmann (2006), Acidity of frozen electrolyte solutions, *J. Phys. Chem. B.*, *110*, 7613–7616.

Satterfiled, C. N., and L. C. Case (1954), Reaction of aldehyde and hydrogen peroxide in aqueous solution—Kinetics of the initial reaction, *Ind. Eng. Chem.*, *46*, 998–1001.

Savarino, J., and M. Legrand (1998), High northern latitude forest fires and vegetation emissions over the last millennium inferred from the chemistry of a central Greenland ice core, *J. Geophys. Res.*, *103*, 8267–8279.

Schade, G. W., R. M. Hofmann, and P. J. Crutzen (1999), CO emissions from degrading plant matter, *Tellus*, *51*, 889–908.

Sigg, A., and A. Neftel (1991), Evidence for a 50% increase in H_2O_2 over the past 200 years from a Greenland ice core, *Nature*, *351*, 557–559.

Spath, B. W., and L. M. Raff (1992), Phenomenological and Monte Carlo models for diffusion-controlled bimolecular reactions in matrices, *J. Phys. Chem.*, *96*, 2179–2185.

Stauffer, B. (2000), Long term climate records from polar ice, *Space Sci. Rev.*, *94*(1–2), 321–336.

Stauffer, B., et al. (1998), Atmospheric CO_2 concentration and millennial-scales climate change during the last glaciation period, *Nature*, *392*, 59–62.

Stauffer, B., J. Fluckiger, E. Monnin, M. Schwander, J. M. Barnola, and J. Chappellaz (2002), Atmospheric CO_2, CH_4 and N_2O records over the past 60,000 years based on the comparison of different polar ice cores, *Ann. Glaciol.*, *35*, 202–208.

Stuart, A. L., and M. Z. Jacobson (2006), A numerical model of the partitioning of trace chemical solutes during drop freezing, *J. Atmos. Chem.*, *53*, 13–42.

Tschumi, J., and B. Stauffer (2000), Reconstructing past atmospheric CO_2 concentration based on ice-core analyses: Open questions due to in situ production of CO_2 in the ice, *J. Glaciol.*, *46*(152), 45–53.

Valentine, E. L., and R. G. Zepp (1993), Formation of carbon monoxide from the photodegradation of terrestrial dissolved organic carbon in natural waters, *Environ. Sci. Technol.*, *27*, 409–412.

Wan, P., and D. Budac (1995), *CRC Handbook of Organic Photochemistry and Photobiology*, pp. 384–392, CRC Press, Boca Raton, Fla.

Wang, H., K. Kawamura, and K. Yamazaki (2006), Water-soluble dicarboxylic acids, ketoacids and dicarbonyls in the atmospheric aerosol over the southern ocean and western Pacific ocean, *J. Atmos. Chem.*, *53*, 43–61.

Wolff, E. W. (1996), Location, movement and reactions of impurities in solid ice, *NATO ASI Ser., Ser. 1*, *43*, 541–560.

Wolff, E. W. (2005), Understanding the past climate history from Antarctica, *Antarct. Sci.*, *17*, 487–495.

Zuo, Y., and R. D. Jones (1996), Formation of carbon monoxide by photolysis of dissolved marine organic material and its significance in the carbon cycling of the oceans, *Geophys. Res. Lett.*, *23*, 2769–2772.

A. J. Colussi, M. I. Guzmán, and M. R. Hoffmann, Environmental Science & Engineering, California Institute of Technology, Pasadena, California 91125, USA. (ajcoluss@caltech.edu)